Size and Strain Rate Effects in Tensile Deformation of Cu Nanowires

Wuwei Liang and Min Zhou†

The George W. Woodruff School of Mechanical Engineering
Georgia Institute of Technology, Atlanta, GA 30332-0405, U.S.A

ABSTRACT

Molecular dynamics simulations with an embedded atom method (EAM)[1] potential are used to analyze the effects of size and strain rate on the tensile deformation of Cu nanowires. The nanowires are single-crystals Cu with 6000 to 96000 atoms. The cross-sectional dimensions of the nanowires vary from 5-20 lattice constants (or 1.8-7.2 nm). The length of the specimens is 60 lattice constants (or 21.6 nm). Deformations under constant strain rates between 1.67×10^{7} and 1.67×10^{9} s^{-1} are analyzed. It is found that the yield stress decreases with specimen size, while increases with loading rate. On the other hand, ductility increases with specimen size and strain rate. The analysis also focuses on the variation of deformation mechanisms with specimen size and strain rate. There is a clear transition in deformation mechanism as specimen size is changed. Specifically, when cross-sectional dimensions are on the order of only a few lattice constants, a combination of twinning and slip is observed. At larger cross-sectional sizes (10-20 lattice constants), crystalline slip is primarily responsible for the progression of plastic deformation. A strong strain rate effect is also seen. As strain rate is decreased, a transition from combined twining and slip to sequential propagation of slip along well-defined and favorably oriented slip planes is observed. At the lower strain rates, a well-structured activation of slip on alternating slip planes is the primary deformation mode.

Keywords: nanowire, size effect, strain rate effect, molecular dynamics

1 INTRODUCTION

The mechanical behavior of nanowires has drawn significant attention in recent years. Experimental and numerical studies have been conducted and reported [2] [3-5]. The deformation of nanowires and atomic systems at finite temperatures in general is an intrinsically dynamic process. Size and strain rate effects arise out of several factors and play important roles in determining the response of nanostructures. For example, the behavior and properties of nanowires are size-dependent due to the discreteness of atomic structures, the length scale (or spatial range) of the atomic interactions, lattice structure, and lattice size scale. The dynamic inertia effect and the finite speeds at which lattice waves propagate also introduce length scales to the problem and contribute to size-dependence of atomic behavior. The inertia effect and finite wave speeds, along with phonon effects, also cause the response of nanostructures to be deformation-rate dependent. Historically and even presently, MD calculations of the mechanical response of atomic systems have been almost exclusively carried out at very high strain rates which are above 10^{9} s^{-1}. This is primarily out of necessity. Specifically, the time steps allowable in MD calculations are limited by the need to resolve high frequency thermal oscillations for atoms and are quite small (on the order of 1 femtosecond). High rates of deformation allow high levels of strain to be reached with practically available computer resources. The use of high deformation rates introduces several issues. First, direct comparisons with experiments are extremely difficult to justify since it is so far not possible to conduct controlled laboratory experiments at high strain rates on nanowires or nano-structures. The artificially high rates also have necessitated computational schemes that allow computations to proceed. One issue is temperature control. Many authors have carried MD simulations of nanowires using the Nose-Hoover thermostat scheme[6, 7] or the velocity scaling scheme which keep the temperature at constant values. If such schemes were not used, the artificially high strain rates would lead to temperatures over the melting point of the system under consideration, invalidating the results and preventing analyses to be carried out. The use of such schemes has allowed results to be obtained and important understandings to be arrived at. However, we note that at the size and time scales of the dynamic deformation of nanowires, there is usually no effective mechanisms for heat to be conducted, convected or radiated out of the system. It is clearly desirable and important to conduct numerical simulations under conditions that do not necessitate artificial schemes for pure numerical reasons. There has been an effort in carrying out simulations at lower strain rates. We describe here some of our recent calculations at strain rates between 10^{7} and 10^{9} s^{-1}. No temperature controlling algorithms are used, providing a more realistic account of the conditions of the dynamic deformation of nanowires. The focus of the analyses is on the size and rate effects on the constitutive

† To whom correspondence should be addressed, Tel: 404-894-3294, Fax: 404-894-0186,
Email: min.zhou@me.gatech.edu

response of Cu nanowires. Parameters varied include loading rate and specimen size.

2 COMPUTATIONAL SETUP

We carried out MD simulations of the simple tension of single crystal Cu nanowires, see Fig. 1. The nanowires have free surfaces in the x- and y-directions. The x-, y-, and z-axes are oriented in the [100], [010], and [001] crystalline directions, respectively. The atoms in the specimens are divided into two types. One is the boundary atoms. Constant velocities $\pm V_0$ (equal magnitude and opposite directions) are maintained for these two planes of atoms, effecting loading necessary for the nanowire to deform at a constant nominal strain rate equal to $\dot{\varepsilon} = 2V_0 / L$. The internal atoms simply deform with the boundary atoms. The system is assigned an initial temperature of 300K and is allowed to relax by holding the length of the wire unchanged and by maintaining a constant temperature using the thermostat procedure. The nanowires are not relaxed to a zero stress state and the beginning of deformation is at stress levels of 0.4-1.6 GPa. The calculations continue with a time step of 1 femtosecond until the nanowire fractures. In contrast to some MD simulations reported in the literature where the Nose-Hoover thermostat procedure was used to maintain a constant temperature, no thermal constraints are applied to the specimen during the calculations here; therefore, the temperature rises adiabatically. This more closely simulates the tensile deformation of a nanowire undergoing high rate deformation.

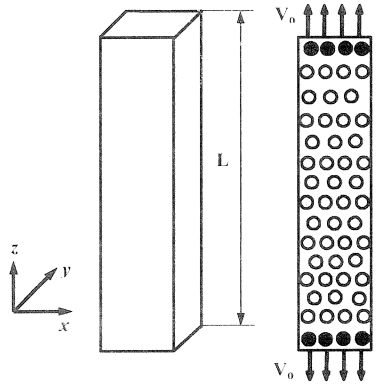

Figure 1: A schematic illustration of the computational model for Cu nanowires. Open circles represent the active atoms and the dark circles represent boundary atoms.

3 RESULTS & DISCUSSION

Figure 2 shows the stress-strain relations of a nanowire at three different strain rates, between $1.67\times10^{7}\mathrm{s}^{-1}$ and $1.67\times10^{9}\mathrm{s}^{-1}$. The cross-sectional dimensions of the nanowire are 5×5 lattice constants (1.8×1.8 nm). The stress-strain relations are essentially linear at small strains. The yield stress is the maximum stress in these cases. The curves for different strain rates coincide during the elastic part of the deformation, indicating rate-independence of elastic deformations which is expected. The curves show a rate-independent Young's modulus of 70 GPa for <001> type crystalline directions. The strain at which yielding occurs increases with strain rate. The yield stress increases from 6.8 GPa to 7.7 GPa as the strain rate increases from $1.67\times10^{7}\mathrm{s}^{-1}$ to $1.67\times10^{9}\mathrm{s}^{-1}$. This dependence of yielding on strain rate is due to the dynamic wave effect or phonon drag that impedes the motion of dislocations. The strain at which ductile rupture occurs increases from 0.2 at $1.67\times10^{7}\mathrm{s}^{-1}$ to 0.32 at$1.67\times10^{9}\mathrm{s}^{-1}$. This strain rate dependence of ductility is consistent with the experimental results reported by [8].

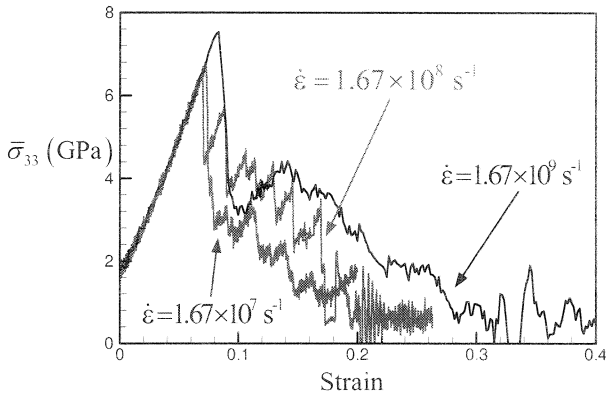

Figure 2: Stress-strain curves of 5×5×60 Cu nanowires at three different strain rates

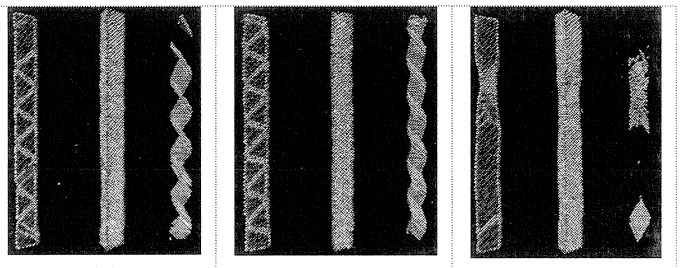

Figure 3: Deformed configurations of Cu nanowires at a strain of 10%; (a) $\dot{\varepsilon}=1.67\times10^{7}\ \mathrm{s}^{-1}$; (b) $\dot{\varepsilon}=1.67\times10^{8}\ \mathrm{s}^{-1}$; and (c) $\dot{\varepsilon}=1.67\times10^{9}\ \mathrm{s}^{-1}$. In each picture, the left image shows an internal cross-section, the center images shows a solid view of the wire with all atoms, and the right image shows only atoms involved in defects. Graphics generated using VMD1.7 [9]

Due to the lack of defects and high strain rates, the yield stress for nanowires undergoing dynamic deformation can far exceed that of bulk Cu. The stress-strain curves in Fig. 1 show precipitous drops in stress after yielding. This sharp drop is caused by the initiation of plastic deformation which occurs at different levels of stress for different strain rates.

Crystalline slip along {111} planes clearly provides the mechanism for the plastic deformation.

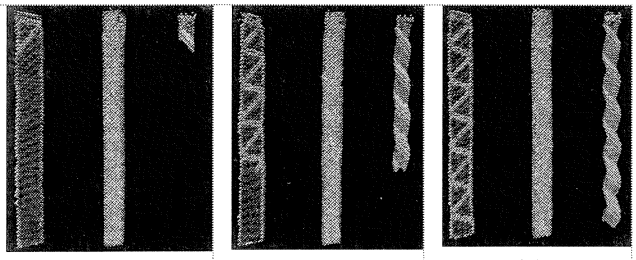

Figure 4: The propagation of slip bands at a strain rate of $1.67\times10^{8}\ s^{-1}$, (a) $\varepsilon = 4.67\%$, (b) $\varepsilon = 5.33\%$, and (c) $\varepsilon = 6.0\%$. The specimen size is 5×5×60.

Activation of multiple slip planes and cross slip are responsible for the formation of the neck in the specimen (Fig. 3(c)). At the strain rate $1.67\times10^{8}\ s^{-1}$, regularly distributed, alternating slip bands are clearly observed throughout the specimen (Fig. 3(a,b)). These slip bands are not simultaneously activated. They propagate from one end to the other within a certain period of time (Fig. 4). This novel phenomenon can be explained by the initially uniform but high strain energy state of the nanowire since it is initially pre-strained with fixed ends. At such state, slip planes are likely to be activated by small thermal or mechanical perturbations. The activation of a slip plane at one location can set off a successive, chain-reaction type activation of slip planes down the specimen. This mechanism of plasticity activation is observed for the strain rates of $1.67\times10^{7}\ s^{-1}$ and $1.67\times10^{8}\ s^{-1}$. The speed at which the active front of the planes propagates along the wire is very high for $\dot{\varepsilon} = 1.67\times10^{7}\ s^{-1}$ and is $271 ms^{-1}$ for $\dot{\varepsilon} = 1.67\times10^{8}\ s^{-1}$. The rapid activation of slip planes across the specimen is responsible for the nearly vertical drop of stress seen following yielding in Fig. 2. The stress-strain curves show oscillatory decreases of stress after the onset of plastic deformation. These oscillations are likely due to successive stages of gradual elastic stretching of temporarily "stationary" lattice structures and rapid plastic slip along the well-defines slip planes. During the elastic stages, straining of the lattice allows strain energy to be accumulated and stored. The stored strain energy allows the activation of slip planes in short, "quick-fire" bursts, leading to relaxation and drop in stress as strain increases. Since specimens deforming at lower strain rates need longer times to "catch up" through further elastic straining, stress decreases are sharper and last longer in time.

The variation of temperature as a function of strain is shown in Fig. 5 for 5×5×60 specimens deformed at different strain rates. The thermal behavior of specimens is similar at the different strain rates. In the elastic deformation stage, temperature decreases slightly as part of the kinetic energy is transformed into potential energy (or strain energy). Subsequently upon yielding, the temperature begins to increase abruptly and continues the upward trend until the nanowires rupture. This temperature increase is primarily due to plastic dissipation but is also due to thermoelastic dissipation at the atomic level. Sharp temperature rises are observed at fracture for $\dot{\varepsilon} = 1.67\times10^{7}\ s^{-1}$ and $\dot{\varepsilon} = 1.67\times10^{8}\ s^{-1}$, primarily because of the conversion of external work to kinetic energy. The gradual increase of temperature for $\dot{\varepsilon} = 1.67\times10^{9}\ s^{-1}$ at late stages of deformation echoes the more ductile and prolonged deformation at this strain rate.

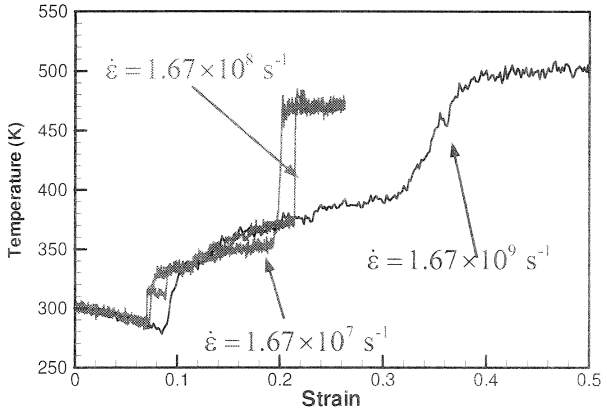

Figure 5: Temperature changes in Cu nanowires of different sizes during the deforming process

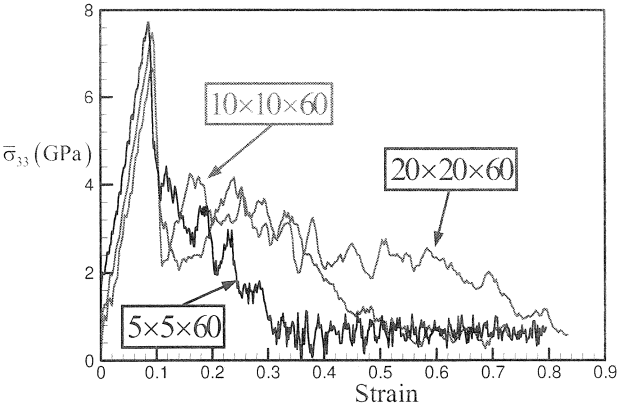

Figure 6: Stress-strain relations for specimens of different sizes, $\dot{\varepsilon} = 1.67\times10^{9}\ s^{-1}$

The effect of specimen size on deformation is also analyzed. Figure 6 shows stress-strain curves for specimens of three different sizes at a strain rate of $1.67\times10^{9}\ s^{-1}$. The cross-sectional dimensions vary from 5 to 20 lattice constants (or 1.8 to 7.2 nm) and the length is 60 lattice constants (21.7 nm) in all cases. Thinner nanowires support higher stresses and the yield stress decreases with specimen size. However, the Young's modulus remains essentially the same for the different sizes, as the initial, elastic portions of the stress-strain curves are essentially parallel to

each other, except for the different amounts of offset at the origin. This offset is due to the uniform pre-stretch applied to the specimens prior to the start of the deformation process. This independence of the Young's modulus on size is different from the findings of [10] who reported that nanowires with larger cross-sections support higher stress levels and have higher values of the Young's modulus. The calculations here also show enhanced ductility at larger sizes. Clearly, this is due to the fact that smaller samples offer fewer opportunities for slip and dislocation motion and larger specimens offer more opportunities for crystalline slip. This effect is clearly seen in Fig. 7. The larger specimen in Fig. 7(c) shows more extensive of slip activation and cross slip.

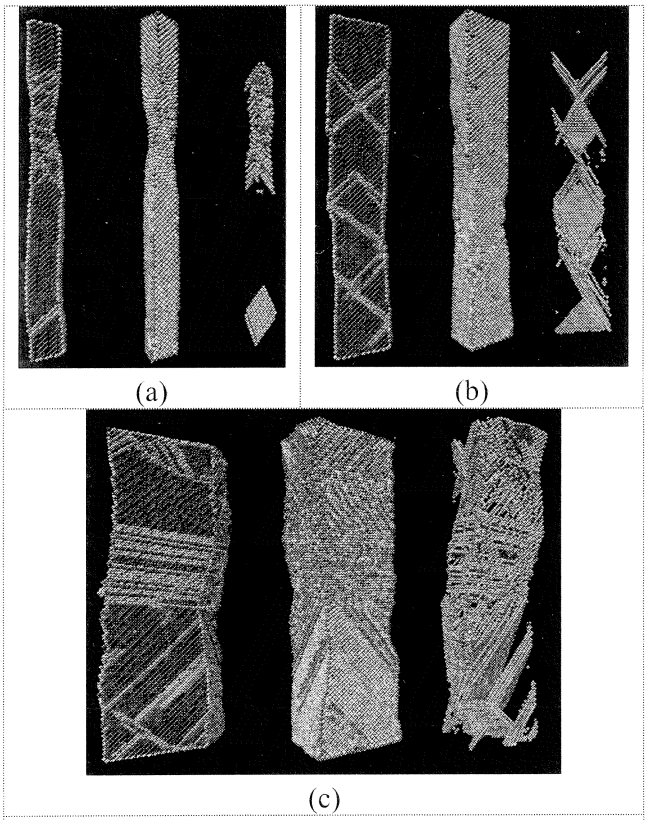

Figure 7: Deformed configurations of Cu nanowires of different sizes ($\dot{\varepsilon} = 1.67 \times 10^{9} s^{-1}$); (a) specimen with a cross-sectional size of 5 lattice spacings ($\varepsilon = 9.17\%$); (b) specimen with a cross-sectional size of 10 lattice spacings, ($\varepsilon = 18.3\%$); and (c) specimen with a cross-sectional size of 20 lattice spacings, ($\varepsilon = 23.3\%$).

4 CONCLUSIONS

Atomistic simulations using embedded atom method were performed for single crystal Cu nanowires. The strain rate and size sale effects were studied. We found that at the elastic deformation stage, the Young's modulus was primarily independent of strain rates and the cross sectional size of specimens. The yield stress (stress at which plastic deformation initiates) decreases with specimen size, while increases with loading rate. On the other hand, ductility increases with specimen size and strain rate. The influences of specimen size are a result of enhanced opportunities for dislocation motion at larger sizes. The influenced of rate are due to the dynamic wave effect or phonon drag that impedes the motion of dislocations.

The analysis also focuses on the variation of deformation mechanisms with specimen size and strain rate. There is a clear transition in deformation mechanism as specimen size is changed. Specifically, when cross-sectional dimensions are on the order of only a few lattice constants, a combination of twinning and slip is observed. At larger cross-sectional sizes (10-20 lattice constants), crystalline slip is primarily responsible for the progression of plastic deformation. Furthermore, a strong strain rate effect is also seen. As strain rate is decreased, a transition of deformation mechanism from combined twining and slip to sequential propagation of slip along well defined and favorably oriented slip planes is observed. Due to the high strain rate, deformation twins are formed during plastic deformation, which serves to reorient the crystal lattice to favor further basal slip. Hence, the combination of twinning and slipping make the specimen more ductile at higher strain rates. The initiation of twins and relaxation of stress make the stress-strain curves display a zigzag of increase and decrease after yielding. At the lower strain rates, a well-structured activation of slip on alternating slip planes is the primary deformation mode.

ACKNOWLEDGEMENTS

This research is supported by NASA Langley Research Center. We would like to thank S. Plimpton for sharing his MD code.

REFERENCES

[1] Daw, M.S. and M.I. Baskes, Physical Review B (Condensed Matter), 29, 6443-53, 1984

[2] Agräit, N., G. Rubio, and S. Vieira, Physical Review Letters, 74, 3995-8, 1995

[3] Ikeda, H., et al., Physical Review letters, 82, 2900-3, 1999

[4] Rubio-Bollinger, G., et al., Physical Review Letters, 87, 026101-1~4, 2001

[5] Mehrez, H. and S. Ciraci, Physical review B, 56, 12632-42, 1997

[6] Nose, S., Mol. Phy., 52, 255-68, 1984

[7] Hoover, W.G., Physical Review A, 31, 1985

[8] Lu, L., S.X. Li, and K. Lu, Scripta Materialia, 45, 1163-69, 2001

[9] Humphrey, W., A. Dalke, and K. Schulten, J. Molec. Graphics, 14, 33-38, 1996

[10] Branício, P.S. and J.-P. Rino, Physical Review B : Condensed Matter, 62, 16950-5, 2000